

# Structure–kinetic relationship study of organozinc reagents†

Cite this: *Chem. Commun.*, 2014, 50, 8709

Received 12th February 2014,  
Accepted 16th May 2014

DOI: 10.1039/c4cc01135j

www.rsc.org/chemcomm

Guanghui Zhang,<sup>ab</sup> Jing Li,<sup>a</sup> Yi Deng,<sup>ab</sup> Jeffrey T. Miller,<sup>b</sup> A. Jeremy Kropf,<sup>a</sup> Emilio E. Bunel<sup>b</sup> and Aiwen Lei<sup>\*abc</sup>

**Phenylzinc reagents prepared from various zinc halides show distinct kinetic features in the palladium-catalyzed Negishi-type oxidative coupling reaction, in which the phenylzinc reagent prepared from ZnI<sub>2</sub> gives the highest rate. *In situ* infrared and X-ray absorption spectroscopy studies show that the higher reaction rate was observed for longer Zn–C bond distances.**

Organozinc compounds were among the first organometallic compounds ever made, among which zinc dialkyls found extensive use as alkylating reagents in organic synthesis, especially in the early development of organometallic chemistry.<sup>1,2</sup> In the past few decades, the discovery of Reformatsky, Simmons–Smith, Fukuyama and Negishi coupling reactions brought organozinc chemistry into its second rapidly developing stage.<sup>3–10</sup> The main challenge in the kinetic investigation of organozinc reagent-involved reactions is that the transmetalation step is usually faster than the other elementary steps in the catalytic cycle. Using Ni-catalyzed oxidative coupling as the kinetic model, the transmetalation of arylzinc with a nickel catalyst has been revealed. This offered an opportunity to quantitatively acquire the kinetic data of the transmetalation of arylzinc reagents.<sup>11</sup> A quantitative kinetic study was also carried out for the transmetalation between an arylzinc reagent and Pd-R.<sup>12</sup> Additionally, in the Ni-catalyzed Negishi-type oxidative homo-coupling reaction, arylzinc reagents prepared by different methods possess very different kinetics due to their varying structural features.<sup>13</sup> The structure of the phenylzinc reagent prepared from the phenyl Grignard reagent has been determined by single crystal analysis; however, the structure of the phenylzinc reagent made from the phenyllithium reagent still remains unknown. Recently, a

combination of nuclear magnetic resonance (NMR), electro-spray ionization (ESI) mass and conductivity measurements have been used to study the structure of phenylzinc reagents, and the presence of lithium zincate complexes has been confirmed.<sup>14–16</sup> Knowledge of the coordination geometry and bond distances is often necessary for a better understanding of the related reaction rates, pathways and selectivity. This is of particular importance for designing new reactions in which organozinc reagents or intermediates are involved. In this communication, we combined *in situ* infrared (IR) and X-ray absorption spectroscopy (XAS) to study the kinetic and structural relationship of phenylzinc reagents prepared from phenyllithium reagents and various zinc halides.

Three different phenylzinc reagents **I**, **II** and **III**, were prepared by mixing phenyllithium reagents with different zinc halides, as shown in Fig. 1. When these phenylzinc reagents were applied in the Pd-catalyzed Negishi-type oxidative homo-coupling reaction, a dramatic difference in the reaction rates was observed. When phenylzinc reagent **I** was used, the reaction was complete within 500 s; while the reaction using

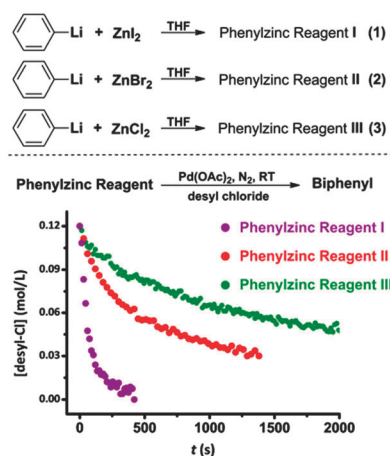


Fig. 1 Synthesis of phenylzinc reagents and the kinetic features of the Pd-catalyzed Negishi-type oxidative homo-coupling reaction.

<sup>a</sup> College of Chemistry and Molecular Sciences, Wuhan University, Wuhan, Hubei 430072, China. E-mail: aiwenlei@whu.edu.cn

<sup>b</sup> Chemical Sciences and Engineering Division, Argonne National Laboratory, 9700 South Cass Avenue, Argonne, IL 60439, USA

<sup>c</sup> State Key Laboratory of Organometallic Chemistry, Shanghai Institute of Organic Chemistry, Chinese Academy of Sciences, 354 Fenglin Lu, Shanghai 200032, China

† Electronic supplementary information (ESI) available: Experimental section and data analysis. See DOI: 10.1039/c4cc01135j

phenylzinc reagent **III** took more than 2000 s. It has previously been demonstrated that transmetalation is the rate-limiting step in the phenylzinc reagent **III**-involved homo-coupling reaction,<sup>12</sup> and further kinetic investigation revealed that transmetalation is also rate-limiting when phenylzinc reagent **I** and **II** are applied (see ESI† for details).

XAS was then used to investigate the structural differences between the three phenylzinc reagents. XAS is a unique and powerful technique for probing the local geometric and electronic structure of metal ions in noncrystalline systems involving solids and liquids, in which the X-ray is able to penetrate the organic solution.<sup>17,18</sup> These advantages make XAS an excellent tool for investigating the structures of organozinc reagents in solution.<sup>19–24</sup>

Zinc iodide adopts a tetrahedral coordination geometry which gives a sharp edge jump originating from the 1s to 4p electron transition in the X-ray absorption near-edge structure (XANES) spectrum.<sup>25</sup> As shown in Fig. 2a, the XANES spectrum of the THF solution of ZnI<sub>2</sub> has similar features to solid ZnI<sub>2</sub>, which indicates the tetrahedral coordination geometry of the Zn species in THF. The shift of the edge energy from 9661.9 eV to 9662.1 eV and the change in shape of the XANES spectrum suggests the coordination of the solvent THF to Zn. Fitting of the extended X-ray absorption fine structure (EXAFS) spectrum suggests that the Zn species in the ZnI<sub>2</sub>/THF solution has two iodide ligands with a bond distance of 2.53 Å and two oxygen ligands at a distance of 2.01 Å, so the structure is assigned as ZnI<sub>2</sub>(THF)<sub>2</sub> (Fig. S1, ESI†). ZnI<sub>2</sub> has 4 iodides coordinated at an average distance of 2.62 Å. It can be seen that the coordination of THF led to a decrease in the Zn–I bond distance. Addition of 1 equivalent of PhLi to the ZnI<sub>2</sub>/THF solution results in a shift of the edge energy to 9660.4 eV. The new species also adopts a tetrahedral coordination geometry, since the shape of the XANES spectrum is still similar to ZnI<sub>2</sub>. The decrease in the height of the “white line” (the sharp intense peak in the rising absorption edge of the XANES spectrum) and the change of the edge energy suggests the coordination of a phenyl anion to Zn. Based on the fitting results of the EXAFS spectrum in Fig. 2b, the major species in phenylzinc reagent **I** is coordinated to two iodides at 2.62 Å, one oxygen atom at 2.09 Å and one carbon anion at 1.96 Å. It is reasonable that the coordination of a

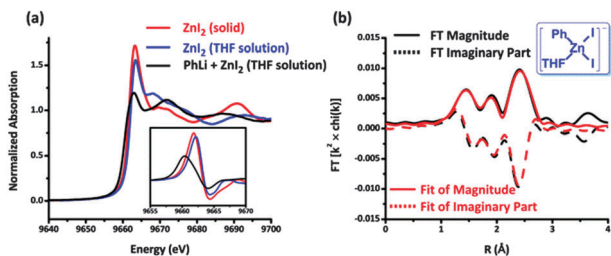


Fig. 2 XAS spectra of phenylzinc reagent **I**. (a) XANES spectra of solid ZnI<sub>2</sub>, ZnI<sub>2</sub>/THF solution and phenylzinc reagent **I**. The inset shows the first derivatives of the XANES spectra. (b) Fitting results of the  $k^2$ -weighted R-space EXAFS spectrum of phenylzinc reagent **I**. FT range: 2.86–10.82 Å<sup>-1</sup>; fitting range: 1.07–2.80 Å.

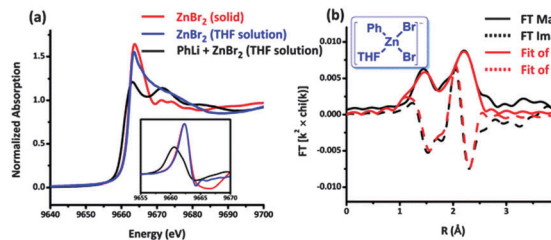


Fig. 3 XAS spectra of phenylzinc reagent **II**. (a) XANES spectra of solid ZnBr<sub>2</sub>, ZnBr<sub>2</sub>/THF solution and phenylzinc reagent **II**. The inset shows the first derivatives of the XANES spectra. (b) Fitting results of the  $k^2$ -weighted R-space EXAFS spectrum of the phenylzinc reagent **II** solution. FT range: 2.66–12.50 Å<sup>-1</sup>; fitting range: 1.12–2.53 Å.

phenyl anion to Zn led to the increase of both the Zn–O and Zn–I bond distances due to electron donation from the phenyl anion to Zn. Although attempts to obtain the single crystal structure of the phenylzinc reagent prepared from PhLi failed, several crystal structures of substituted and very bulky arylzinc iodides have been reported.<sup>26,27</sup> The bond distances that we obtained from XAS are very close to the reported crystal structures. Previous NMR and ESI investigations also suggested that the lithium organozincate monomer complex was the major species under similar conditions,<sup>14</sup> therefore the local structure of phenylzinc reagent **I** was determined as [PhZnI<sub>2</sub>(THF)]<sup>-</sup>.

ZnBr<sub>2</sub> has the same coordination geometry as ZnI<sub>2</sub>, *i.e.*, four bromides are tetrahedrally coordinated to Zn with an average Zn–Br bond distance of 2.42 Å.<sup>25</sup> The edge energy of ZnBr<sub>2</sub> is determined to be 9662.3 eV. As shown in Fig. 3a, coordination of THF to Zn does not change the edge energy, but leads to a change in the shape of the XANES spectrum above the edge, which is similar to ZnI<sub>2</sub>(THF)<sub>2</sub>. For phenylzinc reagent **II**, a decrease of the “white line” height and a shift in the edge were also observed. The formation of the Zn–C bond shifts the edge to a lower energy by 1.7 eV which is the same as the shift from ZnI<sub>2</sub>(THF)<sub>2</sub> to [PhZnI<sub>2</sub>(THF)]<sup>-</sup>. Two bromide anions, one carbon anion and one oxygen atom were found to coordinate to Zn through fitting the EXAFS spectrum (Fig. 3b). The Zn–Br bond distance was determined to be 2.45 Å. The Zn–O and Zn–C bond distances were determined to be 2.11 Å and 1.91 Å, respectively. The local structure of the major species in phenylzinc reagent **II** was thus assigned as [PhZnBr<sub>2</sub>(THF)]<sup>-</sup>. Phenylzinc reagent **III** was also investigated by XAS. As shown in Fig. 4a, the edge energy of ZnCl<sub>2</sub> is 9662.6 eV, which is 0.2 eV higher than the ZnCl<sub>2</sub>/THF solution. The edge energy of phenylzinc reagent **III** is 9660.5 eV, 1.9 eV lower than the ZnCl<sub>2</sub>/THF solution. To summarize all of the XANES results, coordination of THF to zinc halides changes the edge energy. For ZnCl<sub>2</sub>, the shift is –0.2 eV; for ZnI<sub>2</sub>, it is 0.2 eV, but for ZnBr<sub>2</sub>, no shift was observed. Coordination of the phenyl anion to Zn led to an energy shift of –1.7 or –1.9 eV compared with the corresponding ZnX<sub>2</sub>/THF solution.

As shown in Fig. 4b, the EXAFS fitting results suggested a similar structure of phenylzinc reagent **III** to those of **I** and **II**. Two chlorides are bonded at a distance of 2.33 Å, one carbon anion with a bond distance of 1.90 Å and one oxygen atom at

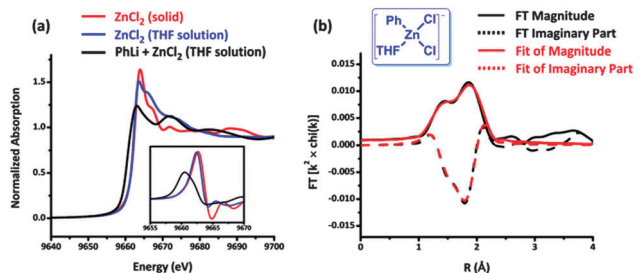


Fig. 4 XAS spectra of phenylzinc reagent III. (a) XANES spectra of solid  $\text{ZnCl}_2$ ,  $\text{ZnCl}_2/\text{THF}$  solution and phenylzinc reagent III. The inset shows the first derivatives of the XANES spectra. (b) Fitting results of the  $k^2$ -weighted R-space EXAFS spectrum of phenylzinc reagent III. FT range:  $2.76\text{--}12.60 \text{ \AA}^{-1}$ ; fitting range:  $1.02\text{--}2.23 \text{ \AA}$ .

Table 1 Summary of the EXAFS fitting results

Phenylzinc reagent	Abs-BS pair <sup>a</sup>	C.N. <sup>b</sup>	$d^c$ (Å)	$\Delta\sigma^{2d}$	$\Delta E_0^e$ (eV)
I	Zn-C	1.3	1.96	0.001	2.32
	Zn-O	1.2	2.09	0.005	-6.06
	Zn-I	2.0	2.62	0.002	-2.12
II	Zn-C	1.0	1.91	0.001	-5.71
	Zn-O	0.8	2.11	0.005	-7.61
	Zn-Br	2.0	2.45	0.003	6.28
III	Zn-C	1.0	1.90	0.001	2.21
	Zn-O	1.0	2.05	0.003	6.45
	Zn-Cl	2.0	2.33	0.001	-7.27

<sup>a</sup> Absorption-backscattering pair. <sup>b</sup> Coordination number ( $\pm 10\%$ ). <sup>c</sup> Bond distance ( $\pm 0.001 \text{ \AA}$ ). <sup>d</sup> Relative Debye-Waller factor to experimental standard. <sup>e</sup>  $E_0$  = threshold energy.

$2.05 \text{ \AA}$  were determined. The EXAFS fitting results of all of the three phenylzinc reagents are summarized in Table 1. The Zn-C bond distance in  $[\text{PhZnI}_2(\text{THF})]^-$  is longer than that in  $[\text{PhZnBr}_2(\text{THF})]^-$ , while  $[\text{PhZnCl}_2(\text{THF})]^-$  has the shortest Zn-C bond distance. The difference between the Zn-C bond distance and the reactivity is probably caused by the electronic properties of the halide ligands. The electronegativity of the halogens increases up the group as a consequence of the halide electronegativity and the availability of their s electrons. In the absence of  $\pi$  interactions between the halide anions and  $\text{Zn}^{2+}$  ( $d^{10}$  electronic configuration), iodide would be expected to donate electron density to the metal through  $\sigma$  interactions. The Zn-C bond will be most weakened by the resulting increase in electron density on  $\text{Zn}^{2+}$ , and therefore the highest transmetallation rate is expected (See ESI† for further discussion).

Combining the structural and kinetic results, it is clear that all of the three phenylzinc reagents form zincate complexes with distorted tetrahedral geometries in THF. The phenyl anion, two halide anions and one THF molecule were found

to coordinate to Zn. The increase in the Zn-C bond distance was observed upon changing the halide anion from chloride to bromide and to iodide. It was also observed that a higher transmetallation rate occurs with longer Zn-C bond distances.

This work was supported by the 973 Program (2012CB725302), the National Natural Science Foundation of China (21390400, 21025206, 21272180 and 21302148), the Research Fund for the Doctoral Program of Higher Education of China (20120141130002) and the Program for Changjiang Scholars and Innovative Research Team in University (IRT1030). Use of the Advanced Photon Source was supported by the U. S. Department of Energy, Office of Science, Office of Basic Energy Sciences, under Contract No. DE-AC02-06CH11357. MRCAT operations were supported by the Department of Energy and the MRCAT member institutions.

## Notes and references

- P. Knochel and R. D. Singer, *Chem. Rev.*, 1993, **93**, 2117-2188.
- P. Knochel, J. J. Almerna Perea and P. Jones, *Tetrahedron*, 1998, **54**, 8275-8319.
- A. Fürstner, *Synthesis*, 1989, 571-590.
- H. Tokuyama, S. Yokoshima, T. Yamashita and T. Fukuyama, *Tetrahedron Lett.*, 1998, **39**, 3189-3192.
- V. B. Phapale and D. J. Cardenas, *Chem. Soc. Rev.*, 2009, **38**, 1598-1607.
- E. Erdik, *Tetrahedron*, 1992, **48**, 9577-9648.
- L. Jin, H. Zhang, P. Li, J. R. Sowa and A. Lei, *J. Am. Chem. Soc.*, 2009, **131**, 9892-9893.
- Q. Liu, Y. Lan, J. Liu, G. Li, Y.-D. Wu and A. Lei, *J. Am. Chem. Soc.*, 2009, **131**, 10201-10210.
- M.-Y. Jin and N. Yoshikai, *J. Org. Chem.*, 2011, **76**, 1972-1978.
- L. Jin, X. Luo and A. Lei, *Acta Chim. Sin.*, 2012, **70**, 1538-1542.
- L. Jin, J. Xin, Z. Huang, J. He and A. Lei, *J. Am. Chem. Soc.*, 2010, **132**, 9607-9609.
- J. Li, L. Jin, C. Liu and A. Lei, *Chem. Commun.*, 2013, **49**, 9615-9617.
- L. Jin, C. Liu, J. Liu, F. Hu, Y. Lan, A. S. Batsanov, J. A. K. Howard, T. B. Marder and A. Lei, *J. Am. Chem. Soc.*, 2009, **131**, 16656-16657.
- J. E. Fleckenstein and K. Koszinowski, *Organometallics*, 2011, **30**, 5018-5026.
- K. Koszinowski and P. Bohrer, *Organometallics*, 2009, **28**, 771-779.
- K. Koszinowski and P. Bohrer, *Organometallics*, 2008, **28**, 100-110.
- R. C. Nelson and J. T. Miller, *Catal. Sci. Technol.*, 2012, **2**, 461-470.
- H. Bertagnolli and T. S. Ertel, *Angew. Chem., Int. Ed.*, 1994, **33**, 45-66.
- A. Sadoc, A. Fontaine, P. Lagarde and D. Raoux, *J. Am. Chem. Soc.*, 1981, **103**, 6287-6290.
- P. Dreier and P. Rabe, *J. Phys. Colloq.*, 1986, **47**, 809-812.
- K. I. Pandya, A. E. Russell, J. McBreen and W. E. O'Grady, *J. Phys. Chem.*, 1995, **99**, 11967-11973.
- M. Uchiyama, Y. Kondo, T. Miura and T. Sakamoto, *J. Am. Chem. Soc.*, 1997, **119**, 12372-12373.
- M. Uchiyama, M. Kameda, O. Mishima, N. Yokoyama, M. Koike, Y. Kondo and T. Sakamoto, *J. Am. Chem. Soc.*, 1998, **120**, 4934-4946.
- P. D'Angelo, A. Zitolo, F. Ceccacci, R. Caminiti and G. Aquilanti, *J. Chem. Phys.*, 2011, **135**, 154509.
- C. Chieh and M. A. White, *Z. Kristallogr.*, 1984, **166**, 189-197.
- Z. Zhu, M. Brynda, R. J. Wright, R. C. Fischer, W. A. Merrill, E. Rivard, R. Wolf, J. C. Fettingier, M. M. Olmstead and P. P. Power, *J. Am. Chem. Soc.*, 2007, **129**, 10847-10857.
- Y. Wang, B. Quillian, C. S. Wannere, P. Wei, P. v. R. Schleyer and G. H. Robinson, *Organometallics*, 2007, **26**, 3054-3056.